Multifidelity, Multidisciplinary Design Under Uncertainty with Non-Intrusive Polynomial Chaos

Thomas K. West IV* and Clyde Gumbert†
NASA Langley Research Center, Hampton, VA, 23681

The primary objective of this work is to develop an approach for multifidelity uncertainty quantification and to lay the framework for future design under uncertainty efforts. In this study, multifidelity is used to describe both the fidelity of the modeling of the physical systems, as well as the difference in the uncertainty in each of the models. For computational efficiency, a multifidelity surrogate modeling approach based on non-intrusive polynomial chaos using the point-collocation technique is developed for the treatment of both multifidelity modeling and multifidelity uncertainty modeling. Two stochastic model problems are used to demonstrate the developed methodologies: a transonic airfoil model and multidisciplinary aircraft analysis model. The results of both showed the multifidelity modeling approach was able to predict the output uncertainty predicted by the high-fidelity model as a significant reduction in computational cost.

Nomenclature

C	Additive Correction	R	Stochastic Response
D	Design Variables	r	Polynomial Order of the Correction
J	Optimization Objective	α	Polynomial Chaos Expansion Coefficient
N_s	Number of Samples	μ	Mean
N_t	Number of Terms in a Total-Order Polynomial Chaos Expansion	Ψ	Random Basis Function
		ϕ	Model Roll Angle
n	Number of Random Dimensions	σ	Standard Deviation
P_f	Probability of Failure	ξ	Standard Input Random Variable
q	Polynomial Order		

I. Introduction

As computational resources become increasingly more powerful, there is a strong push to move higher fidelity modeling into conceptual design. While many high-fidelity analysis tools, such as Large Eddy Simulations for aerodynamics, may still be too expensive to conduct a full vehicle configuration design, mixing a few results from high-fidelity models with cheaper, low-fidelity models is an attractive alternative to greatly improving predictions in conceptual design over using strictly low-fidelity tools, such as empirical models and engineering methods.

The challenge in a multifidelity approach is dealing with the uncertainty in each of the levels of fidelity. While many simple approaches exist for comparing the outputs from models of varying fidelity, prediction of uncertainty is generally ignored or the uncertainty in the low-fidelity model is used as the uncertainty measure, as it is less computationally demanding than using the high-fidelity model to quantify uncertainty. This can have a significant impact on the actual uncertainty amount. An approach to quantifying the uncertainty in a multifidelity model is needed to address uncertainty in each level of fidelity and combine them into one prediction of output uncertainty that can be efficiently used in a design under uncertainty setting. The objectives of this work are to describe the uncertainty sources in multifidelity modeling, introduce an approach for quantifying uncertainty in multifidelity models, and to demonstrate multifidelity,

*Aerospace Engineer, Vehicle Analysis Branch, Systems Analysis and Concepts Directorate, Member AIAA.
†Aerospace Engineer, Vehicle Analysis Branch, Systems Analysis and Concepts Directorate.

multidisciplinary uncertainty quantification (UQ). This is all done to lay the foundation for future design under uncertainty efforts.

Few approaches actually exist for quantifying uncertainty in multifidelity models as the use of classical sampling techniques (e.g., Monte Carlo) do not lend themselves easily to account for the different levels of fidelity and are computationally very expensive. Surrogate model based approaches allow for the differentiation of multiple fidelity levels and are attractive for computational savings. Work by Shah et al.[1] used output space mapping to correct low fidelity surrogate models, which were used for efficient aerodynamic shape optimization. Forrester et al.[2] developed an approach based on Gaussian Process or Kriging to correlate multiple data sets of different levels of fidelity, which has been named Co-Kriging. In the area of polynomial chaos, Ng and Eldred[3] introduced the idea of correcting a low-fidelity polynomial chaos expansion (PCE), but had limitations due to the use of sparse grids estimating the PCE coefficients. The goal and primary contributions of this work will be to build on this previous work and make the approach more tractable to a wider variety of applications by using a regression approach for estimating the PCE coefficients and allowing for different uncertainties to exist between a low-fidelity and a high-fidelity model. Additionally, this work will apply a multifidelity approach in a multidisciplinary aircraft analysis, which has not previously been attempted in the presence of uncertainty.

The next section describes the sources of uncertainty in multi-fidelity modeling and design under uncertainty problem formulation. Section III describes the approach for multifidelity surrogate modeling using non-intrusive polynomial chaos. Section IV applies the method to two stochastic problems. The last section provides a brief summary of this work and discusses important findings.

II. Uncertainty in Multifidelity Models

This section describes the uncertainty that may exist in multifidelity analysis. First a description of the types of uncertainty in numerical modeling is provided, followed by a description of uncertainty in multifidelity problems. The last section describes performing design optimization under the presence of uncertainty for completeness.

A. Types of Uncertainty in Numerical Modeling

A critical step in any uncertainty analysis is the classification of the uncertain parameters. These parameters may be mathematically represented differently based on the nature of their uncertainty. Incorrect classification and/or treatment of uncertain parameters can result in widely varying output uncertainty.

Two main types of uncertainty exist in numerical modeling: aleatory uncertainty and epistemic uncertainty.[4] Aleatory uncertainty is the inherent variation of a physical system. Such variation is due to the random nature of input data and can be mathematically represented by a probability density function if substantial experimental data is available for estimating the distribution type. An example of this type of uncertainty could be the fluctuations in freestream quantities. While still considered random variables, these variations are not controllable and are sometimes referred to as irreducible uncertainties.

Epistemic uncertainty in a stochastic problem comes from several potential sources. These include a lack of knowledge or incomplete information of the behavior of a particular variable. Also, ignorance or negligence with regards to accurate treatment of model parameters is a source of epistemic uncertainty. Contrary to aleatory uncertainty, epistemic uncertainty is sometimes referred to as reducible uncertainty. An increase in knowledge regarding the physics of a problem, along with accurate modeling, can reduce the amount of this type of uncertainty, but typically comes at some cost. Epistemic uncertainty is typically modeled using intervals because the use of probabilistic distributions (even a uniform distribution) can lead to inaccurate predictions in the amount of uncertainty in a system. Upper and lower bounds of these intervals can be drawn from limited experimental data or from expert predictions and judgment.[5,6]

An additional, special case of epistemic uncertainty is numerical error. This uncertainty is common in numerical modeling and is defined as a recognizable deficiency in any phase or activity of modeling and simulations that is not due to lack of knowledge of the physical system. In CFD, an example of this type of uncertainty would be the discretization error in both the temporal and spatial domains that comes from the numerical solution of the partial differential equations that govern the system.[6] This uncertainty can be well understood and controlled through code verification and grid convergence studies.

B. Multifidelity Model Uncertainty

In multifidelity analysis, the objective is to predict the output of a high-fidelity model by using a combination of low and high-fidelity predictions. When uncertainty is accounted for in the analysis, the term "multifidelity" can have two meanings that need to be investigated. The most common being multifidelity mathematics or physics modeling. The second is multifidelity uncertainty modeling. The latter is important because it can have a different impact on predictions from models of different modeling fidelity and/or models of different fidelity can have different sources of uncertainty.

The real challenge is dealing with this difference in uncertainty. While each may have a series of input uncertainties which, again, may be the same or different, each model will have a different amount of model-form uncertainty. This is illustrated in Figure 1 by comparing the sources of uncertainty in low and high-fidelity models to some known truth.

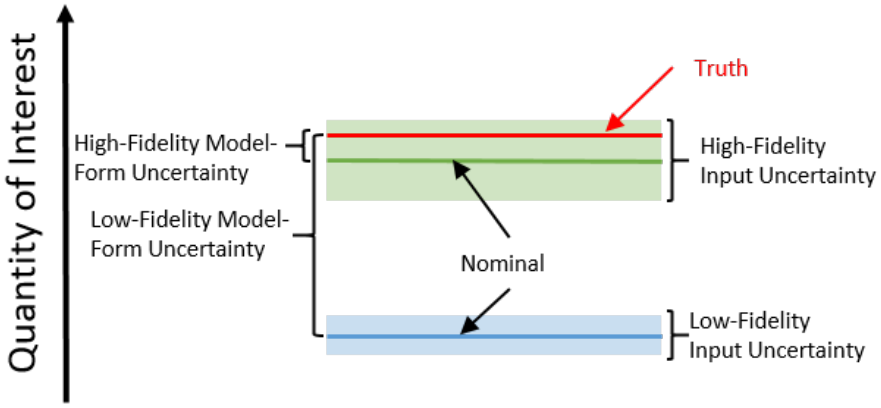

Figure 1: Example of uncertainty in a multi-fidelity analysis.

From Figure 1, notice that the illustration shows that the amount of input uncertainty is larger for the high-fidelity model. In general, this may be expected. Typically, higher-fidelity models have more inputs, more tunable parameters and, possibly, more numerical error. Consider a comparison between a computational fluid dynamics model and an engineering correlation. However, regardless of the impact of input uncertainty on each level of fidelity, the model-form uncertainty is going to be greater in lower fidelity models.

The issue with model-form uncertainty is that without some truth (e.g., experimental data), measuring this uncertainty may be challenging, or even impossible. In the cases where there is no truth available, the only measure of model-form uncertainty is between the different levels of fidelity, which requires that the high-fidelity model be known as a "better" approximation. When using multifidelity analysis for UQ, accurately quantifying both the input and, if possible, the model-form uncertainties is necessary to ensure accurate uncertainty predictions. This involves quantifying the uncertainty that is common between the levels of fidelity, as well as any uncertainty that is possessed by the different models.

C. Design Under Uncertainty

In classical design optimization, the typical objective is to minimize some quantity, F, subject to a series of constraints on either the design variables or quantities impacted by changing the design variables. An example of this type of optimization may be to minimize the drag on a wing subject to maintaining prescribed lift and moment values. For a stochastic process, however, the objective is a function of uncertainty in addition to the design variables, which could actually possess uncertainty as well. The challenge is how to design a component or system in the presence of this uncertainty as part of the optimization process.

There are two primary objectives to design under uncertainty. The first is referred to as reliability-based design. In this problem, the objective to minimize some quantify of interest, J, (e.g., drag) subject to meeting a probability of failure requirement, $\tilde{P}_f$, as shown in the optimization program in Eq. (2) where F is a quantity of interest for measuring reliability. For the wing example, this constraint may be that the wing structure must have a reliability of 99% probability any component of the wing will not yield.

$$\min J \tag{1}$$

$$\text{subject to: } P_f(F) \leq \tilde{P}_f \tag{2}$$

Another objective for designing under uncertainty is called robust design. In this problem, the objective is to design a system that is robust to any uncertainty. This is accomplished by formulating an objective that is a function of the statistics of the design quantity, such as the mean and variance. An example objective is shown in Eq. (3).

$$\min J = \mu_F + w\sigma_F \tag{3}$$

In this objective, the goal is to minimize both the mean of the quantity, μ_F, and improve robustness by reducing the standard deviation, σ_F. The scale or weight factor, w, is used to scale the standard deviation to control the bias of the objective. Note that this formulation is only suitable for problems with only aleatory uncertainty. An alternative measure must be used when epistemic uncertainty is present. This is discussed by Shah et al.[1]

When using gradient-based optimization, the robust objective, J requires more careful treatment. The gradient of the robust objective with respect to the design variables , $\mathbf{D}$, is shown in Eq. (4). Obtaining the derivatives of the moments can be computationally demanding, which may make gradient-based optimization expensive for problems with a large number of random variables, without the use of an adjoint method.

$$\frac{dJ}{d\mathbf{D}} = \frac{d\mu_F}{d\mathbf{D}} + w\frac{d\sigma_F}{d\mathbf{D}} \tag{4}$$

III. Multifidelity Polynomial Chaos Expansions

This section outlines the approach for multifidelity modeling and UQ using non-intrusive polynomial chaos. First, generalized polynomial chaos is discussed, followed by a discussion of the point-collocation approach to estimating the expansion coefficients. Next, the multifidelity approach is introduced and a simple example problem is used to demonstrate the applicability. Lastly, the discussion of moments and moment gradients is given for completeness.

A. Generalized Polynomial Chaos

Polynomial chaos is a surrogate modeling technique based on the spectral representation of the uncertainty. An important aspect of spectral representations is the decomposition of a response value or random function R into a linear combination of separable deterministic and stochastic components, as shown in Eq. (5).

$$R(\boldsymbol{D}, \boldsymbol{\xi}) \approx P_{q,n} = \sum_{i=0}^{N_t-1} \alpha_i(\boldsymbol{D})\Psi_i(\boldsymbol{\xi}) \tag{5}$$

Here, α_i is the deterministic component and Ψ_i is the random variable basis functions corresponding to the i^{th} mode. The basis functions, Ψ_i, of each random variable are determined using the Askey key[7] and are dependent on the distribution of each random variable. The response, R, is a function of independent, deterministic variables, $\mathbf{x}$, and n independent, standard random variables, $\boldsymbol{\xi}$. Note that this series is, by definition, an infinite series; however, in practice, it is truncated and a discrete sum is taken over a number of output modes. To form a complete basis or a total order expansion, N_t terms are required, which can be computed from Eq. (6) for a polynomial chaos expansion (PCE) of order q and a number of random dimensions or variables, n.

$$N_t = \frac{(n+q)!}{n!q!} \tag{6}$$

Further details on polynomial chaos theory are given by Eldred[8] and Ghanem.[9]

B. Point-Collocation, Non-Intrusive Polynomial Chaos

The objective with any PCE method is to determine the expansion coefficients, α_i. To do this, polynomial chaos methods can be implemented using an intrusive or a non-intrusive approach. While an intrusive method may appear straightforward in theory, for complex problems this process may be time consuming, expensive, and difficult to implement.[5] In contrast, the non-intrusive approach can be easily implemented to construct a surrogate model that represents a complex computational simulation, because no modification to the deterministic model is required. The non-intrusive methods require only the response (or sensitivity)[10–12] values at selected sample points to approximate the stochastic response surface.

Several methods have been developed for non-intrusive polynomial chaos (NIPC). Of these, the point-collocation NIPC method has been used extensively in many aerospace simulations and CFD problems[6,10,13,14] for improved computational efficiency and tractability for high-dimension problems over other spectral projection based approaches. The point-collocation method starts with replacing a stochastic response or random function with its PCE by using Eq. (5). Then, N_t sample vectors are chosen in random space and the deterministic code is evaluated at these points, which is the left hand side of Eq. (5). Following this, a linear system of N_t equations can be formulated and solved for the expansion coefficients of the PCE. This system is shown in Eq. (7).

$$\begin{pmatrix} R(\mathbf{D},\boldsymbol{\xi}_0) \\ R(\mathbf{D},\boldsymbol{\xi}_1) \\ \vdots \\ R(\mathbf{D},\boldsymbol{\xi}_P) \end{pmatrix} = \begin{pmatrix} \Psi_0(\boldsymbol{\xi}_0) & \Psi_1(\boldsymbol{\xi}_0) & \cdots & \Psi_P(\boldsymbol{\xi}_0) \\ \Psi_0(\boldsymbol{\xi}_1) & \Psi_1(\boldsymbol{\xi}_1) & \cdots & \Psi_P(\boldsymbol{\xi}_1) \\ \vdots & \vdots & \ddots & \vdots \\ \Psi_0(\boldsymbol{\xi}_P) & \Psi_1(\boldsymbol{\xi}_P) & \cdots & \Psi_P(\boldsymbol{\xi}_P) \end{pmatrix} \begin{pmatrix} \alpha_0 \\ \alpha_1 \\ \vdots \\ \alpha_P \end{pmatrix} \tag{7}$$

Note that for this linear system, N_t is the minimum number of deterministic samples required to obtain a direct solution. If more samples are available and are linearly independent, the system is considered overdetermined and can be solved using a least squares approach. The number of samples over the required minimum is represented by the use of an oversampling ratio (OSR), defined as the ratio of number of actual samples to the minimum number required (i.e., N_t). In general, the number of collocation points can be determined by multiplying Eq. (6) by an OSR. Hosder et al.[15] determined that the PCE is dependent on the number of collocation points and an effective OSR of two for the stochastic model problems studied.

C. Multifidelity Polynomial Chaos Expansions

In multifidelity analysis, the goal is to predict the output from a high-fidelity model, R_H, by correcting outputs from a low-fidelity model, R_L. With polynomial chaos, one approach is to correct a PCE of the low-fidelity model and a minimal amount of training points from the high-fidelity model.

One approach to correcting a low-fidelity model is to use an additive correction, as shown in Eq. (8) for a number of random dimensions n and a low-fidelity model PCE, $P_{q,n}$, of order q.

$$R_H = R_L + C \approx P_{q,n} + C \tag{8}$$

For simplicity, first assume the low and high-fidelity models are assumed to have the same number of random dimensions, n. (The relaxation of this assumption is discussed later.) The PCE of the low-fidelity model, $P_{q,n}$, is corrected by adding C. Rearranging Eq. (8), the correction term C can be approximated by Eq. (9), which is a PCE of order r, where $r < q$. Note that if $r \not< q$, a PCE of order q could be fit to the high-fidelity model, which would be defeat the purpose of a multifidelity model.

$$C = R_H - R_L \approx P_{q-r,n} \tag{9}$$

Using this formulation, Eq. (8) can be rewritten in terms of the PCE coefficients and basis functions, as shown in Eq. (10).

$$R_H \approx P_{q,n} + P_{q-r,n} = \sum_{\beta \in \{\beta \,:\, \sum_{j=1}^{n} i_j \le r\}} (\alpha_{L\beta} + \alpha_{C\beta})\Psi_\beta(\vec{\xi}) + \sum_{\beta \in \{\beta \,:\, r < \sum_{j=1}^{n} i_j \le q\}} \alpha_{L\beta}\Psi_\beta(\vec{\xi}) \tag{10}$$

where,

$$\beta = (i_1, ..., i_n) \tag{11}$$

and

$$i_k = 0, 1, 2, 3, ... \quad \text{for} \quad k = 1, ..., n \tag{12}$$

Here, the set β is used to identify the order of each variable. For example, $\beta = (1, 0, 1)$ would indicate the term that is first order in variable one and first order in variable three. To understand this expansion, each term can be looked at individually. The first term on the RHS states that the expansion coefficients of the PCE representing the low-fidelity model, α_L, are corrected by adding the expansion coefficients, α_C, of the PCE representing the correction, C, to each common term, up to order r. The second term leaves the remaining higher order terms unchanged from the original, low-fidelity model PCE as there is not enough information to correct terms above order r. Recall that the order of the correction is less than the order of the fit for the low-fidelity model.

With this approach, the expectation is the low-fidelity model is able to capture the underlying trend of the response as a function of the random variables and also that higher order contributions, above that of the order of the correction PCE, are minimal or at least well described by the low-fidelity model. After constructing this multifidelity surrogate model, the uncertainty in the models can then be efficiently propagated through the surrogate to obtain an output uncertainty estimate.

The approach can be extended by relaxing the previous assumption that the random variables are the same between the low and high-fidelity models, labeled here as n_L and n_H. If the high-fidelity model possesses random variables in addition to those in the low-fidelity model, the correction term must span the domain of ξ_H for which $\xi_L \in \xi_H$. This results in an additional term being added to Eq. (10) that contains the terms in the correction that do not have a like term in the low-fidelity model.

$$\begin{aligned} R_H \approx P_{q,n} + P_{q-r,n} = & \sum_{\beta \in \{\beta \,:\, \sum_{j=1}^{n_L} i_j \leq r\}} (\alpha_{L\beta} + \alpha_{C\beta}) \Psi_\beta(\vec{\xi}) + \sum_{\beta \in \{\beta \,:\, r < \sum_{j=1}^{n_L} i_j \leq q\}} \alpha_{L\beta} \Psi_\beta(\vec{\xi}) + \\ & \sum_{\gamma \in \{\gamma \,:\, \sum_{j=1}^{n_H} i_j \leq r\}} \alpha_{C\gamma} \Psi_\gamma(\vec{\xi}) \end{aligned} \tag{13}$$

where,

$$\beta = (i_1, ..., i_{nL}), \quad \gamma = (i_{nL+1}, ..., i_{nH}) \tag{14}$$

and

$$i_k = 0, 1, 2, 3, ... \quad \text{for} \quad k = 1, ..., n_H \tag{15}$$

Careful consideration should be given to the number of samples needed to construct the low-fidelity model PCE and the correction PCE. As previously stated, the order of C should not meet or exceed the order used for R_L as this would eliminate the need for a multifidelity model. However, with this dimension expansion, the correction term could be fit to any order in the variables not common between the low and high-fidelity models by adding only enough samples to capture the non-interaction terms. The caution is just noted here that any practitioner should be mindful of the number of samples of each level of fidelity as to not waste resources or possibly degrade accuracy.

D. Moments and Design Variable Sensitivities

To facilitate design under uncertainty with gradient-based optimization, statistical moments and gradient information with respect to the design variables must be determined. Eldred et al.[8] shows that with polynomial chaos, moments can be determined analytically, as shown in Eqs. (16) and (17) for the mean and variance of the stochastic expansion.

$$\mu_R = \langle R \rangle \approx \sum_{i=0}^{P} \alpha_i(\boldsymbol{D}) \langle \Psi_i(\boldsymbol{\xi}) \rangle = \alpha_0 \tag{16}$$

$$\sigma_R^2 = \langle (R - \mu_R)^2 \rangle \approx \langle (\sum_{i=0}^{P} \alpha_i(\boldsymbol{D}) \Psi_i(\boldsymbol{\xi}))^2 \rangle = \sum_{i=1}^{P} \alpha_i^2(\boldsymbol{D}) \langle \Psi_i^2(\boldsymbol{\xi}) \rangle \tag{17}$$

The robust design objective in Eq. (3) can be calculated with these two moments. To satisfy the adjoint-based design objective in Eq. (4), the sensitivities of moments must be obtained. The sensitivity of the mean with respect to the design variables is obtained by differentiating Eq. (16), which is shown in Eq. (18).

$$\frac{d\mu_R}{dD} = \frac{d}{dD}\langle R \rangle = \langle \frac{dR}{dD} \rangle \tag{18}$$

This calculation is trivial when the sensitivities of each response with respect to each design variable are known, as it is simply the average of the sensitivities for each design variable. The sensitivity of the variance is shown in Eq. (19), which is obtained by differentiating Eq. (17).

$$\frac{d\sigma_R^2}{d\boldsymbol{D}} = \sum_{i=1}^{P} \langle \Psi_i^2(\boldsymbol{\xi}) \rangle \frac{d\alpha_j^2}{d\boldsymbol{D}} = 2 \sum_{i=1}^{P} \alpha_j \langle \Psi_i^2(\boldsymbol{\xi}) \rangle \frac{d\alpha_j}{d\boldsymbol{D}} \tag{19}$$

Obtaining the sensitivities in Eq. (19) requires that the sensitivities of the expansion coefficients be determined. A second polynomial chaos expansion can be constructed by differentiating Eq. (5) with respect to the j^{th} design variable, as shown in Eq. (20).

$$\frac{\partial R(\boldsymbol{D}, \boldsymbol{\xi})}{\partial D_j} \approx \sum_{i=0}^{P} \frac{d\alpha_i(\boldsymbol{D})}{dD_j} \Psi_i(\boldsymbol{\xi}) \tag{20}$$

Solving this equation for the sensitivities of the expansion coefficients must be done for each of the design variable and can be accomplished with general point-collocation or an L_1-minimization approach,[18] if the system is underdetermined. A gradient-enhanced point-collocation[10] approach can also be used, but has an added cost of obtaining the mixed derivative $\frac{\partial}{\partial \boldsymbol{\xi}}(\frac{\partial R}{\partial \boldsymbol{D}})$.

IV. Applications

To demonstrate multifidelity UQ using the above NIPC-based approach, two stochastic problems are investigated. First is the analysis of an airfoil using two levels of fidelity. Next, the analysis of a multidisciplinary aircraft configuration was conducted. The remainder of this section details each of these model problems, there sources of uncertainty, and the benefits of using multifidelity UQ.

A. Airfoil Model

To demonstrate the multifidelity PCE approach, consider the computational fluid dynamics (CFD) model of drag on a NACA 0012 airfoil in transonic flow. The Mach number and angle of attack were selected as 0.8 and 1.25 degrees, respectively. The flow was modeled as inviscid and solved by using Standford University's SU2[16] with second order spatial discretization and the JST flux scheme.

Sources of uncertainty considered in this model came from inherent variations in Mach number and angle of attack. Both were assumed to be normally distributed. The Mach number had a mean of 0.8 with a standard deviation of 0.005, while the angle of attack had a mean of 1.25 with a standard deviation of 0.1 degrees. This uncertainty is consistent with previous work.[17] Based on Eq. (6), a second order PCE of the drag would have six terms and would require a minimum of six evaluations of the deterministic model to estimate the expansion coefficients by using a point collocation approach. A comparison of the surface pressure coefficients on four grid levels is shown in Figure 2(a) and a contour Mach number is shown in Figure 2(b) for the finest grid. Notice that the lowest grid resolution is completely unable to detect the presence of both upper and lower surface shock waves.

In this problem, the low and high-fidelity models are selected with different grid resolutions. The low-fidelity model had grid dimensions of 50x50 and the high-fidelity model had grid dimensions of 400x400. The computational time between these two differ from about three seconds to nearly three minutes per solution on the same number of CPUs and computer hardware. The uncertainty in the Mach number and angle of attack was propagated through each fidelity level separately to illustrate the difference in output uncertainty and provide a "truth" to compare the multifidelity model. The drag coefficient values and 95% confidence intervals are shown in Figure 3.

Notice that the low-fidelity model underpredicts the amount of uncertainty in the drag coefficient by nearly 50%. For this problem, the underprediction is not unexpected as a low grid resolution may not be

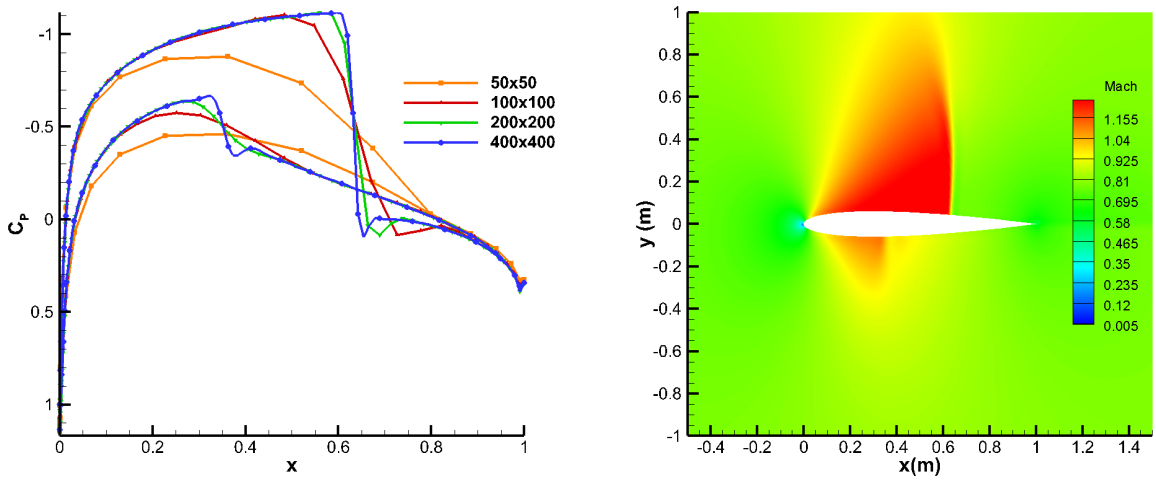

(a) Surface pressure coefficient distributions for multiple grid levels.

(b) Mach contour of the finest grid solution.

Figure 2: NACA 0012 transonic flow solution.

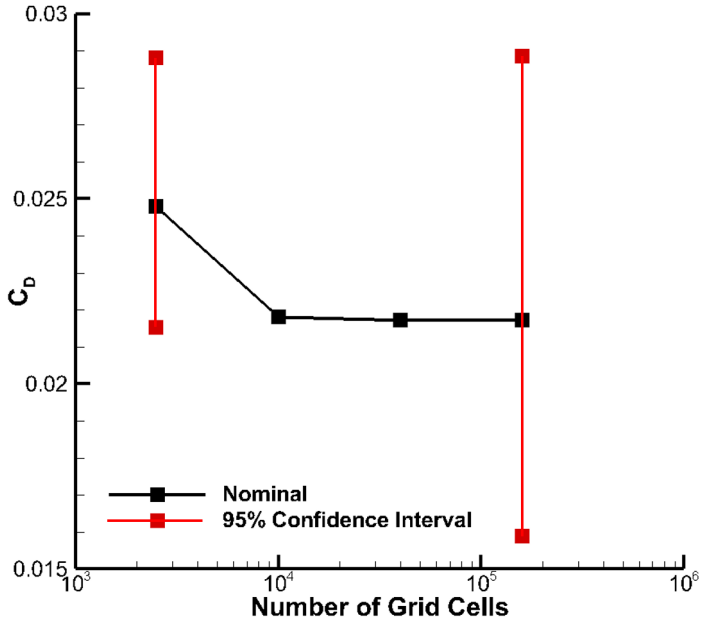

Figure 3: Comparison of low an high-fidelity models.

sensitive to perturbations as features in the boundary layer and/or near the shock may be missed. Note that there is NOT less uncertainty in the low-fidelity model. While Figure 3 shows that there is less input uncertainty, the model-form uncertainty is much greater. This is important to understand as ignoring the model-form component could be misleading.

Construction of a second order PCE with the high-fidelity model took about 18 minutes (minimum of six sample points). Using the low-fidelity model, the cost is about 18 seconds. The goal with the multifidelity

PCE is to obtain nearly the same prediction as shown for the high-fidelity model uncertainty, but at a lower computational cost.

Because a second order fit is being used for the low-fidelity model, there are two choices for the order of the correction: a constant value (zeroth order) or first order. A constant correction would only require one evaluation of the high-fidelity model; however, this is dangerous for two reasons. The first is where to pick that one point. The difference between the two levels of fidelity is likely not constant across the domain of the random variables. The second issue is that correcting only the constant term of the low-fidelity model, only moves the mean. The uncertainty would remain the same as the constant term is not dependent on the uncertain variables.

A first order correction would require a minimum of three evaluations of the high-fidelity model. Using the additive approach outlined in the previous section, the multifidelity model can be constructed and the uncertainty can be propagated efficiently through the model by using a Monte Carlo sample approach. The 95% confidence intervals of the low, high, and multifidelity models are shown in Figure 4. Notice that the multifidelity model is able to predict nearly the same amount of uncertainty as the high-fidelity model with only three evaluations of the high-fidelity model. In terms of time, six low-fidelity plus three high-fidelity model evaluations take about just over nine minutes, which is about half the computational time compared to using only the high-fidelity model. This is a great result given the significant difference in the physics that are captured between the two levels of fidelity.

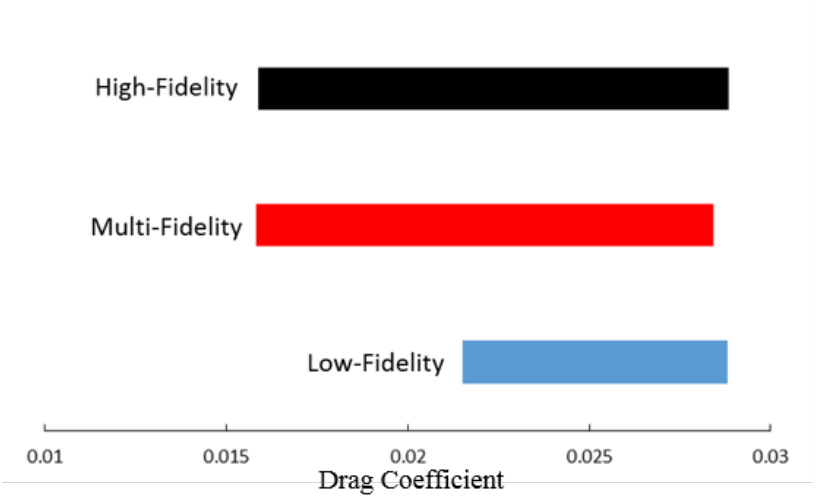

Figure 4: 95% confidence intervals of the low, high, and multtfidelity models.

B. Aircraft Model

To further demonstrate multifidelity UQ with NIPC, a multidisciplinary aircraft model was investigated. The baseline configuration of this model is shown in Figure 5. The analysis of this aircraft is composed of four primary discipline models: geometry, aerodynamics, performance, and structures. The data paths from each discipline to another is the most difficult portion of the modeling to formulate, particularly inside an UQ setting. This has to be done in such a way to minimize an loss of information or, in the context of uncertainty, the introduction of additional model-form uncertainty. To simplify the problem, the entire analysis loop is treated as a "black box". This removes the need to directly pass uncertainty information from one discipline to the next. While this approach could, in theory, reduce the number of evaluations of each discipline, special treatment of the interdisciplinary uncertainty is required and may introduce error.

The geometry was modeled and altered during design by using OpenVSP v3.9.1.[19] With this module, variations to the baseline geometry were passed into OpenVSP in batch mode and the new geometry is returned including the necessary meshes for the aerodynamic analysis.

The aerodynamic analysis of the aircraft was the multifidelity part of the model. The low-fidelity model was a vortex lattice method (VLM) used in VSPAero v3.1. Spatial convergence studies of the structured grid of the vehicle in many possible configurations (i.e., within the limits of the design variables to be discussed later) were performed to ensure minimal convergence error. The high-fidelity model was selected

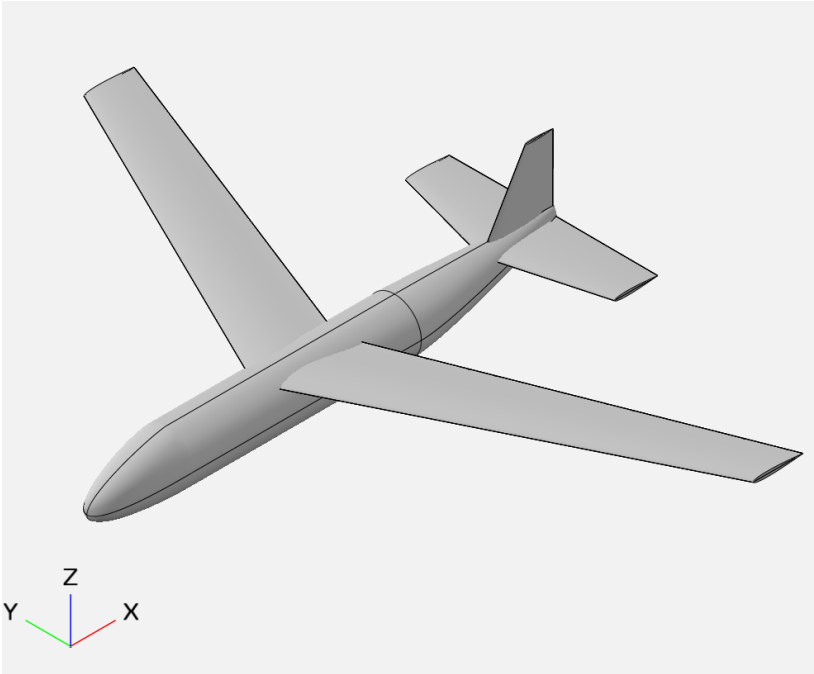

Figure 5: Baseline aircraft configuration.

as CART3D. Similarly, spatial convergence studies of the surface and flow field meshes were performed with the vehicle in a variety of configurations. Figures of the surface meshes of the baseline configurations are shown in Figures 6(a) and 6(b). These two models differ in the physics they model and the assumptions of the flow. Also, notice that in VSPAero, only the wing and horizontal surface were being modeled as apposed to the full aircraft being modeled in CART3D. Analyzing only the wing is typical in conceptual design. A parasite drag factor is added to the drag predicted for the wing with the VLM.

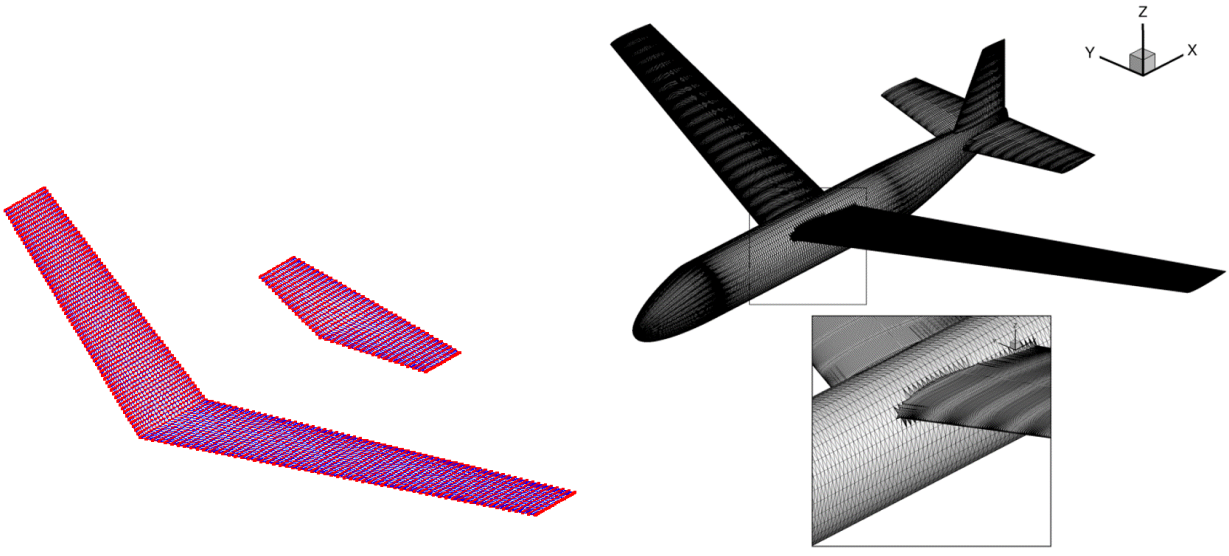

(a) VSPAero mesh.

(b) CART3D mesh.

Figure 6: Aerodynamic analysis computational meshes.

For performance, the aircraft was trimmed for steady flight using a body fixed reference frame. Forcing the aircraft to trim requires multiple runs of the aerodynamic analysis. The approach in this study was to

generate a polar, spline the wing-body axial force, normal force, and moment to be interpolated on during root finding process required to determine the trim angle of attack, thrust required, and lift of the tail.

Lastly, the structural model is an in-house, structural analysis code currently being developed at NASA Langley. Structural line models and beam based sizing methods are used for efficient analysis at what is deemed to be around a low- to mid-fidelity analysis. This physics-based tool is designed for rapid structural sizing and internal layout of the wings, fuselage, and tail components. Here the aircraft is assumed to be an all aluminum structure. The sizing is done to prevent any yielding of any member and satisfies minimum gauge requirements. After the trim angle of attack is determined, loads from the aerodynamics analysis are passed to the structural model for sizing.

Further information on each of these models are left to the provided references as their details are beyond the focus of this work. Note, however, that the process shown here is very general and any of these models could be replaced by another. The UQ process is independent of what happens inside the "black-box", which is a key benefit of this approach.

The flight conditions for the model were a 10 deg. flight path angle at 38,000 feet and a Mach number of 0.5. and the aircraft had a specified maximum gross weight and maximum thrust. As for uncertainty, the low-fidelity model (the model that uses VSPAero for the aerodynamic analysis) two sources of uncertainty were identified: the location of the center of gravity (CG) and Mach number both with covariances of 1%. For the high-fidelity model (the model that uses CART3D for the aerodynamic analysis) two additional uncertainty sources were included: the modulus of aluminum with a covariance of 5% and an uncertainty factor in the predicted trim angle of attack with a covariance of 5%. These additional parameters adds a level of fidelity to the uncertainty problem, in addition to the multifidelity physics modeling. Note that each of these parameters is used by different disciplines in the analysis. Aerodynamics and the trim analysis both depend on Mach number. The trim analysis and the structures model depend on the CG location, while the modulus and trim angle uncertainty are only needed by the structures model.

The uncertainty in this model was propagated through to determine the uncertainty in the payload the aircraft can carry and the amount of excess thrust available. These quantities represent those that may be used as objectives or constraints in future optimization problems. For each quantity of interest, a second order PCE was fit to the two variables, low-fidelity model. A first order fit was used for the correction fit for each of the random parameters. The 95% confidence intervals of each are shown in Figures 7(a) and 7(b). In total, this required a minimum of six evaluations of the low-fidelity model and five evaluations of the high-fidelity model. Note that if only the high-fidelity model was used, at least 15 evaluations would be needed.

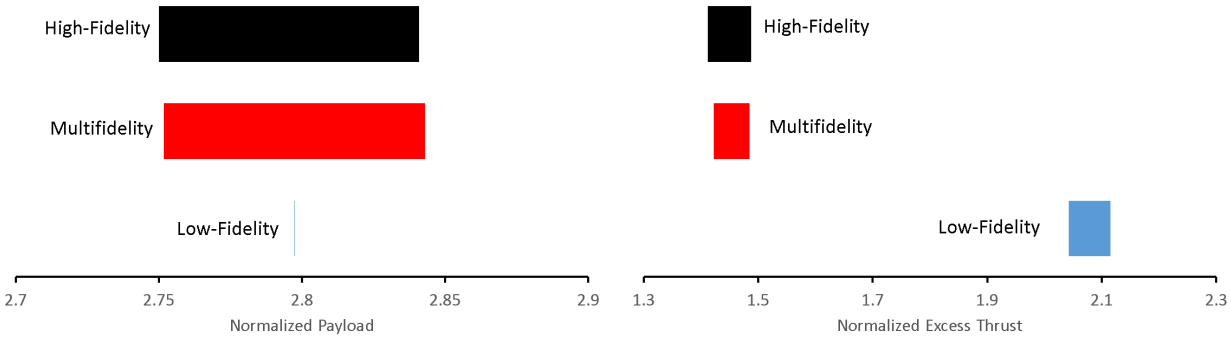

(a) Normalized payload.

(b) Normalized excess thrust.

Figure 7: Aircraft model payload and thrust 95% confidence intervals.

This model produces very interesting results. First, notice that the payload prediction using the low-fidelity model is basically insensitive to the input uncertainty. This is expected given the very small amount of uncertainty in the Mach number and CG location. However, the uncertainty in the modulus of aluminum contributes significantly in the high-fidelity model. The multifidelity model was able to capture this significant difference by accurately producing only a very small difference in the confidence interval estimates compared to the high-fidelity model.

Similarly, the excess thrust prediction shows a large discrepancy between the predictions from the different levels of fidelity, even though their interval widths are comparable. This is because the additional sources of uncertainty in the high-fidelity model do not contribute significantly to the output variance. However, there is a large model-form uncertainty component here that the multifidelity model is able to rectify.

V. Conclusions

Moving higher-fidelity modeling and uncertainty quantification into conceptual design and analysis is the next step to reducing costs and improving the capability to investigate novel vehicle configurations. While an abrupt shift to the use of the highest fidelity models may not yet be practical, blending cheaper, low-fidelity tools with more expensive, high-fidelity, models is the first step towards improved accuracy. In this study, a surrogate-based, multifidelity uncertainty quantification approach was outlined for quantifying input uncertainty between models of varying fidelity both in the mathematical modeling and the input uncertainty. Demonstration on two stochastic model problems was carried out and demonstrated the true capability of this approach as the results highlighted how uncertainty can differ between levels of fidelity and how a multifidelity model could be used to accurately predict the uncertainty in a high-fidelity model. All of this work is done in setting up the foundation for design under uncertainty using multifidelity modeling. Future work will focus on extending the ideas in this paper to more complex models, with much more uncertainty and then inserting the approach into an optimization environment.

References

[1]Shah, H. R., Hosder, S., Koziel, S., Tesfahunegn, Y. A., and Leifsson, L., "Multi-fidelity Robust Aerodynamic Design Optimization Under Mixed Uncertainty," AIAA Paper 2015-0917, 2015.

[2]Forrester, A. I., Sóbester, A., and Keane, A. J., "Multi-fidelity optimization via surrogate modelling," *Proceedings of the Royal Society of London A: Mathematical, Physical and Engineering Sciences*, Vol. 463, No. 2088, 2007, pp. 3251–3269.

[3]Ng, L. W. T. and Eldred, M. S., "Multifidelity Uncertainty Quantification Using Non-Intrusive Polynomial Chaos and Stochastic Collocation," AIAA Paper 2012-1852, 2012.

[4]Oberkampf, W., Helton, J., and Sentz, K., "Mathematical representation of uncertainty," AIAA Paper 2001-1645, June 2001.

[5]Hosder, S. and Bettis, B., "Uncertainty and sensitivity analysis for reentry flows with inherent and model-form uncertainties," *Journal of Spacecraft and Rockets*, Vol. 49, No. 2, 2012, pp. 193–206.

[6]Bettis, B., Hosder, S., and Winter, T., "Efficient Uncertainty Quantification in Multidisciplinary Analysis of a Reusable Launch Vehicle," AIAA Paper 2011-2393, April 2011.

[7]Xiu, D. and Karniadakis, G. E., "The Wiener–Askey Polynomial Chaos for Stochastic Differential Equations," *SIAM Journal on Scientific Computing*, Vol. 24, No. 2, 2002, pp. 619–644.

[8]Eldred, M. S., "Recent Advances in Non-Intrusive Polynomial Chaos and Stochastic Collocation Methods for Uncertainty Analysis and Design," AIAA Paper 2009-2274, May 2009.

[9]Ghanem, R. G. and Spanos, P. D., *Stochastic Finite Elements: A Spectral Approach*, Springer-Verlag, New York, 1991.

[10]West IV, T. K., Hosder, S., and Johnston, C. O., "Multi-Step Uncertainty Quantification Approach Applied to Hypersonic Reentry Flows," *Journal of Spacecraft and Rockets*, Vol. 51, No. 1, 2014, pp. 296–310.

[11]Lockwood, B. and Mavriplis, D., "Gradient-Based Methods for Uncertainty Quantification in Hypersonic Flows," *Computers and Fluids Journal*, Vol. 85, Oct. 2013, pp. 27–38.

[12]Roderick, O., Anitescu, M., and Fischer, P., "Polynomial Regression Approaches Using Derivative Information for Uncertainty Quantification," *Nuclear Science and Engineering*, Vol. 164, No. 2, 2010, pp. 122–139.

[13]Hosder, S., Walters, R. W., and Balch, M., "Point-Collocation Nonintrusive Polynomial Chaos Method for Stochastic Computational Fluid Dynamics," *AIAA Journal*, Vol. 48, No. 12, 2010, pp. 2721–2730.

[14]Han, D. and Hosder, S., "Inherent and Model-Form Uncertainty Analysis for CFD Simulation of Synthetic Jet Actuators," AIAA Paper 2012-0082, Jan. 2012.

[15]Hosder, S., Walters, R. W., and Balch, M., "Efficient Sampling for Non-Intrusive Polynomial Chaos Applications with Multiple Uncertain Input Variables," AIAA Paper 2007-0125, 2007.

[16]Economon, T. D., Palacios, F., Copeland, S. R., Lukaczyk, T. W., and Alonso, J. J., "SU2: An Open–Source Suite for Multiphysics Simulation and Design," *AIAA Journal*, Vol. 54, No. 3, 2016, pp. 828–846.

[17]Shah, H. R., Hosder, S., and Winter, T., "A Mixed Uncertainty Quantification Approach with Evidence Theory and Stochastic Expansions," AIAA Paper 2014-0298, 2014.

[18]West IV, T. K. and Hosder, S., "Uncertainty Quantification of Hypersonic Reentry Flows with Sparse Sampling and Stochastic Expansions," *Journal of Spacecraft and Rockets*, Vol. 52, No. 1, 2015, pp. 120–133.

[19]Hahn, A., "Vehicle Sketch Pad: A Parametric Geometry Modeler for Conceptual Aircraft Design," AIAA Paper 2010-0657, 2010.

[20]"Dakota, A Multilevel Parallel Object-Oriented Framework for Design Optimization, Parameter Estimation, Uncertainty Quantification, and Sensitivity Analysis: Version 6.4 Users Manual," Tech. rep., SAND2014-4633, 2014.